AIAA JOURNAL
Vol. 36, No. 1, January 1998

# Multigrid Method for the Euler and Navier–Stokes Equations

A. O. Demuren* and S. O. Ibraheem†
*Old Dominion University, Norfolk, Virginia 23529*

**Results are presented of a study to implement convergence acceleration techniques based on the multigrid concept in a three-dimensional computer code developed for solving Euler and Navier–Stokes equations. The multigrid method implemented is the full approximation storage–full multigrid algorithm, which is applicable to nonlinear equations. Multigrid convergence estimates based on a single-grid or bigrid stability analysis are performed. The latter was found to yield a better prediction of practical multigrid convergence rates. In typical applications, for both laminar and turbulent flows, savings of up to 50% in CPU time were obtained with the multigrid implementation.**

## Nomenclature

| | |
|---|---|
| $A, B, C$ | = inviscid flux Jacobians |
| $\boldsymbol{E}, \boldsymbol{F}, \boldsymbol{G}$ | = conserved inviscid flux vectors |
| $\boldsymbol{E}_v, \boldsymbol{F}_v, \boldsymbol{G}_v$ | = viscous flux vectors |
| $\boldsymbol{e}$ | = error vector |
| $e_0$ | = total specific internal energy |
| $g$ | = computational grid in the multigrid sequence |
| $I$ | = $\sqrt{-1}$ |
| $I_h^H$ | = restriction operator |
| $I_H^h$ | = interpolation operator |
| $\boldsymbol{I}$ | = identity matrix |
| $J$ | = transformation Jacobian |
| $K$ | = coarse grid correction matrix |
| $\hat{K}, \hat{L}, \hat{N}$ | = Fourier symbols |
| $k$ | = turbulent kinetic energy |
| $L_1, L_2, L_3$ | = alternating direction implicit operators |
| $M$ | = bigrid amplification matrix |
| $Ma$ | = Mach number |
| $P$ | = forcing term in multigrid procedure |
| $p$ | = pressure |
| $\boldsymbol{Q}$ | = solution vector |
| $\boldsymbol{R}$ | = residual vector |
| $Re$ | = Reynolds number |
| $R_0, R_1, R_2, S_0, S_1, S_2, Y_0, Y_1, Y_2$ | = viscous flux Jacobians |
| $S_1, S_2$ | = relaxation or smoothing operator |
| $t$ | = time |
| $\boldsymbol{U}_0$ | = constant amplitude vector |
| $u, v, w$ | = velocity components |
| $x, y, z$ | = Cartesian coordinates |
| $\gamma$ | = specific heat capacity ratio |
| $\Delta$ | = incremental change |
| $\delta_x, \delta_y, \delta_z$ | = finite difference operators |
| $\varepsilon$ | = dissipation rate of turbulent kinetic energy |
| $\varepsilon_i, \varepsilon_e$ | = coefficients of implicit and explicit artificial dissipation |
| $\theta_x, \theta_y, \theta_z$ | = Fourier modes in $x$, $y$, and $z$ direction |
| $\lambda$ | = amplification factor |
| $\lambda_{\mu-\mathrm{bg}}$ | = bigrid amplification factor |
| $\lambda_{\mu-\mathrm{sg}}$ | = smoothing factor |
| $\mu_t, k_t$ | = eddy and thermal viscosity |
| $\nu^1, \nu^2$ | = pre- and postrelaxation counters |
| $\xi, \eta, \zeta$ | = computational coordinate system |
| $\rho$ | = density |
| $\rho_{\mathrm{mg}}$ | = multigrid convergence factor |

*Subscripts and Superscripts*

| | |
|---|---|
| $h, H$ | = fine and coarse grid levels |
| $n, n_1, n_2$ | = time step or iteration number |

Presented as Paper 96-6299 at the AIAA 34th Aerospace Sciences Conference, Reno, NV, Jan. 15–19, 1996; received June 6, 1996; revision received May 26, 1997; accepted for publication Sept. 29, 1997. 

*Professor, Department of Mechanical Engineering. Associate Fellow AIAA.

†Research Assistant, Department of Mechanical Engineering; currently Research Associate, Oil and Gas Unit, 204 Hosler Building, Pennsylvania State University, University Park, PA 16802.

## Introduction

COMPUTATIONAL fluid dynamics methods are now routinely applied to study many complex flow phenomena that are difficult or even impossible to study experimentally. For flows with engineering significance, solution of the full Navier–Stokes equations, or more precisely, the Reynolds-averaged form, have been found to yield realistic simulations of flow characteristics and heat transfer. However, even for the time-averaged approximation, the computational cost is often too expensive where quantitative accuracy is required. To reduce cost, acceleration techniques such as residual smoothing, local time stepping, enthalpy damping, and multigrid are introduced. Thus far, multigrid is considered the most effective, especially when used to solve strongly elliptic problems where only a few iterations are needed for convergence. Structurally, multigrid algorithms iterate on a hierarchy of successively coarser grids to accelerate convergence on the finest grid.

Multiple grids were first proposed in the form of two-grid level schemes to accelerate the convergence of iterative procedures by Southwell[1] and Stiefel,[2] among others. Full multiple grid methods were introduced for the Poisson equation by Federenko,[3] and the approach was generalized by Bakhalov[4] to any second-order elliptic operator with continuous coefficients. Perhaps the most influential work on the application of multigrid methods to elliptic type problems is by Brandt,[5] who also introduced the use of local mode analysis to determine the smoothing rates of multigrid schemes. Multigrid acceleration was also successfully applied to the transonic potential flow equation, which is of mixed elliptic–hyperbolic type, by South and Brandt,[6] Jameson,[7] McCarthy and Reyhner,[8] and a host of others. More recently, multigrid methods were applied to the Euler equations by Jameson,[9] Mulder,[10] and Anderson et al.[11]

Many practical problems require the solution of the Navier–Stokes equations. Apart from the obvious difficulties of the treatment of viscous terms and the implementation of a turbulence model, it is usually necessary to cluster grids near walls, to resolve the boundary layer. This increases the stiffness of the system of equations and slows down the convergence rate of many iterative schemes. The specific objective of this work is to develop an efficient multigrid algorithm to solve steady-state problems governed by the two- and three-dimensional compressible Navier–Stokes equations. The multigrid method is implemented in the two- and three-dimensional versions of the Proteus computer code,[12,13] although

the results presented would be for the latter only. Furthermore, the efficiency of the implemented multigrid procedure will be demonstrated by application of the code to several test problems and also by comparison with stability analysis predictions.

## Basic Governing Equations

The basic governing equations are the Reynolds-averaged conservation equations for compressible Navier–Stokes equations in three dimensions. In generalized curvilinear coordinates, the equations can be written in strong conservation law form using vector notation as

$$\frac{\partial \boldsymbol{Q}}{\partial t} + \frac{\partial(\boldsymbol{E}-\boldsymbol{E}_v)}{\partial \xi} + \frac{\partial(\boldsymbol{F}-\boldsymbol{F}_v)}{\partial \eta} + \frac{\partial(\boldsymbol{G}-\boldsymbol{G}_v)}{\partial \zeta} = 0 \qquad (1)$$

where the conserved variables of vector $\boldsymbol{Q}$ are defined as

$$\boldsymbol{Q} = (1/J)[\rho, \rho u, \rho v, \rho w, \rho e_0]^T \qquad (2)$$

In addition to the preceding equations, an equation of state is required to link the pressure to the dependent variables. The ideal gas law is chosen; for calorically perfect gases, it can be written as

$$p = (\gamma - 1)\left[\rho e_0 - \tfrac{1}{2}\rho(u^2 + v^2 + w^2)\right] \qquad (3)$$

## Solution Methods

The governing equations are solved by marching in time from some known set of initial conditions using a finite difference technique. The time differencing method used is the generalized scheme of Beam and Warming,[14] in which the viscous fluxes are split directionally. The implicit Beam–Warming alternating direction implicit (ADI) scheme applied to the preceding Navier–Stokes equations can be written in the following quasilinear form[15]:

$$\begin{aligned}
&[\boldsymbol{I} + \Delta t(\delta_x A - \delta_{xx} R_0 - \varepsilon_i \boldsymbol{I}\Delta x \delta_{xx})][\boldsymbol{I} + \Delta t(\delta_y B - \delta_{yy} S_0 \\
&\quad - \varepsilon_i \boldsymbol{I}\Delta y \delta_{yy})][\boldsymbol{I} + \Delta t(\delta_z C - \delta_{zz} Y_0 - \varepsilon_i \boldsymbol{I}\Delta z \delta_{zz})]\Delta Q \\
&\quad = -\Delta t[A\delta_x - R_0\delta_{xx} - R_1\delta_{yx} - R_2\delta_{zx} + B\delta_y - S_1\delta_{xy} \\
&\quad - S_0\delta_{yy} - S_2\delta_{zy} + C\delta_z - Y_1\delta_{xz} - Y_2\delta_{yz} - Y_0\delta_{zz} \\
&\quad + \varepsilon_e \boldsymbol{I}(\Delta x^3\delta_{xxxx} + \Delta y^3\delta_{yyyy} + \Delta z^3\delta_{zzzz})]Q
\end{aligned} \qquad (4)$$

To solve the governing equations, an evenly spaced grid is defined in the computational $(\xi, \eta, \zeta)$coordinate system. Spatial derivatives in Eq. (4) are approximated by second-order finite difference formulas. With this central difference formulation, high-frequency instabilities can appear as the solution develops. For example, in high Reynolds number flows, oscillations can result from the odd–even decoupling inherent in the use of second-order central differencing. In addition, physical phenomena such as shock waves can cause instabilities when they are captured by a finite difference algorithm. Artificial viscosity, or dissipation, is normally added to the solution algorithm to suppress these high-frequency instabilities. Two artificial viscosity models are considered in this study: a constant coefficient model used by Steger[16] and the nonlinear coefficients model of Jameson et al.[17]

The turbulent Reynolds stress tensor resulting from time averaging is assumed proportional to the rate of strain tensor, with the coefficient of proportionality defined as the eddy viscosity $\mu_t$. Similarly, turbulent heat fluxes are assumed to be proportional to the temperature gradient vector, with the coefficient of proportionality defined as the turbulent thermal diffusivity $k_t$. These turbulence coefficients are computed in this study using the low Reynolds number $k$–$\varepsilon$ model proposed by Chien.[18]

In the approximate factorization form presented in Eq. (4) the left-hand side is split into a three-sweep sequence such that each sweep requires only the solution of a series of 5 × 5 block-tridiagonal systems, which are efficiently solved using the Thomas algorithm.

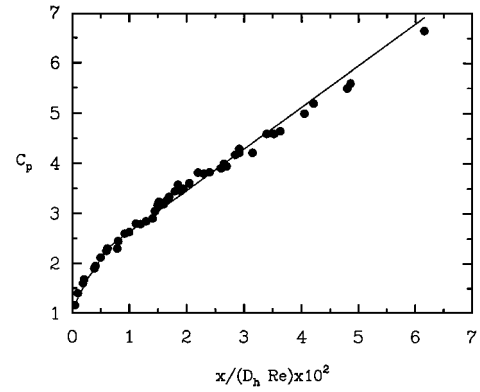


**a) Static pressure coefficient for laminar flow for the rectangular duct experiment of Sparrow et al.[20]**

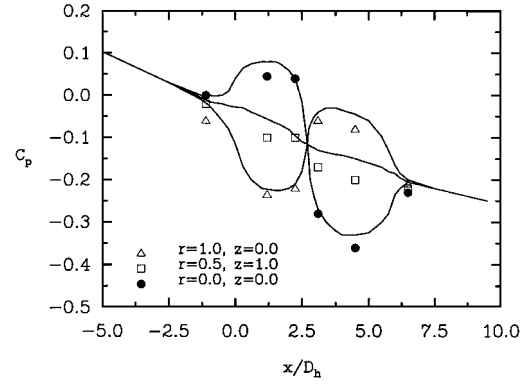


**b) Static pressure coefficient for the S-duct experiment of Taylor et al.[21]**

**Fig. 1 Comparison of MG computations (lines) with experimental data (symbols).**

## Multigrid Full Approximation Storage–Full Multigrid Scheme

A multigrid procedure has been developed to accelerate the convergence of the Beam–Warming ADI numerical scheme described in the preceding section. The multigrid algorithm adopted is the full approximation storage–full multigrid method (FAS–FMG), which is applicable to nonlinear systems of equations.

The ADI scheme can be written in the operator form

$$L_1 L_2 L_3 \Delta \boldsymbol{Q} = -\Delta t \boldsymbol{R} \qquad (5)$$

A simple multigrid cycle is performed as follows.

1) Solve Eq. (5) on the finest grid $g^h$, i.e.,

$$L_1^h L_2^h L_3^h \Delta Q^h = -\Delta t R^h \qquad (6)$$

2) Compute the flowfield at the present time step:

$$(Q^{n+1})^h = (Q^n)^h + (\Delta Q^n)^h \qquad (7)$$

3) Compute the residual $R^h$ from the right-hand side of Eq. (4).

4) Transfer the flow variables $Q^h$ and residual $R^h$ to grid $g^{2h}$ and compute the forcing terms $P^{2h}$as follows:

$$P^{2h} = I_h^{2h} R^h - R^{2h}(Q^{2h}) \qquad (8)$$

5) Then, the coarse grid $g^{2h}$ problem, driven by the forcing terms, is solved as

$$L_1^{2h} L_2^{2h} L_3^{2h} \Delta Q^{2h} = \Delta t\left[R^{2h}(Q^{2h}) + I_h^{2h} R^h - R^{2h}\left(I_h^{2h} Q^h\right)\right] \qquad (9)$$

6) Steps 3–5 are repeated recursively on $g^{4h}$, $g^{8h}$, etc., to solve for the corrections, and the cumulative corrections are interpolated on to the fine grid and added to the solution, until the finest grid $g^h$; for example,

$$\begin{aligned}
Q^{2h} &\leftarrow Q^{2h} + I_{4h}^{2h}\left(Q^{4h} - I_{2h}^{4h} Q^{2h}\right) \\
Q^h &\leftarrow Q^h + I_{2h}^h\left(Q^{2h} - I_h^{2h} Q^h\right)
\end{aligned} \qquad (10)$$

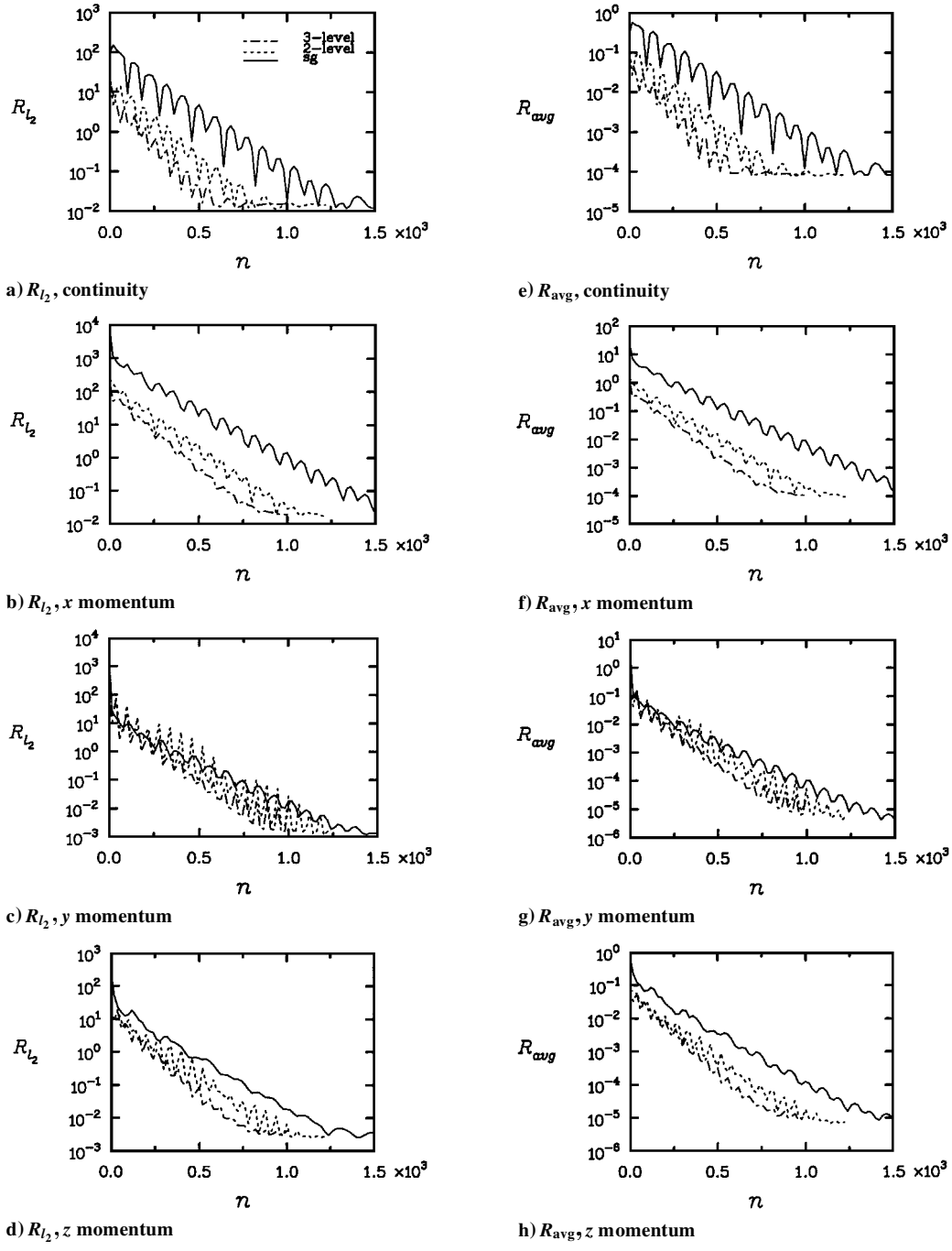


a) $R_{l_2}$, continuity

e) $R_{\text{avg}}$, continuity

b) $R_{l_2}$, $x$ momentum

f) $R_{\text{avg}}$, $x$ momentum

c) $R_{l_2}$, $y$ momentum

g) $R_{\text{avg}}$, $y$ momentum

d) $R_{l_2}$, $z$ momentum

h) $R_{\text{avg}}$, $z$ momentum

**Fig. 2 Convergence history for three-dimensional duct flow, second-order boundary conditions, 41 × 21 × 21 coarse grid.**

These steps are repeated on the fine grid until $R^h = 0$ or a predetermined tolerance level because we are interested only in steady-state solutions. Depending on the schedule for the grids and the order in which they are visited, the multigrid structure may take the form of a simple V cycle or more complicated ones like the full multigrid V cycle or the W cycle. In the present study, the full multigrid V cycle is utilized throughout.

In general, one iteration is performed on the finest grid, one on intermediate grids, and four on the coarsest grid. But on coarser grids, the computational work is successively reduced by a factor of 4 for two dimensions and by a factor of 8 for three dimensions. This implies that the computational work units (relative to a single grid iteration on the finest grid) for a three-level multigrid cycle is $1\frac{3}{4}$ for two dimensions and $1\frac{5}{16}$ for three dimensions. Additional overheads for intergrid transfers, generation of grids and calculation of metrics on coarser grids, calculation of residuals, etc., raise the total work units to about $2\frac{5}{8}$ and 2, respectively, for two- and three-dimensional multigrid procedures. That is, the multigrid convergence rate must be faster by at least these factors for there to be a saving in CPU time. One method for reducing the relative overhead of the multigrid procedure is to perform more fine grid iterations per multigrid (MG) cycle, e.g., three iterations on the finest grid instead on one. Then the effective total work units per MG cycle are reduced to 2 and $1\frac{5}{8}$, respectively. Preliminary tests showed that the latter approach is better for two-dimensional computations, whereas the former approach is better for the three-dimensional computations. In the two-dimensional case, the slower convergence rate resulting from performing a MG cycle only every third fine-grid iteration is more than compensated for by the cheaper overall MG overhead, whereas in the three-dimensional case, where the MG overhead costs are lower, the faster convergence rate of performing one MG cycle per fine-grid iteration is dominant. These approaches are mostly used in the results presented in subsequent sections.

## Convergence Characteristics

Although multigrid methods are becoming very popular, only a few works have studied their stability in practical problems. Both the smoothing factor based on a conventional von Neumann stability analysis and the amplification factor based on the bigrid stability

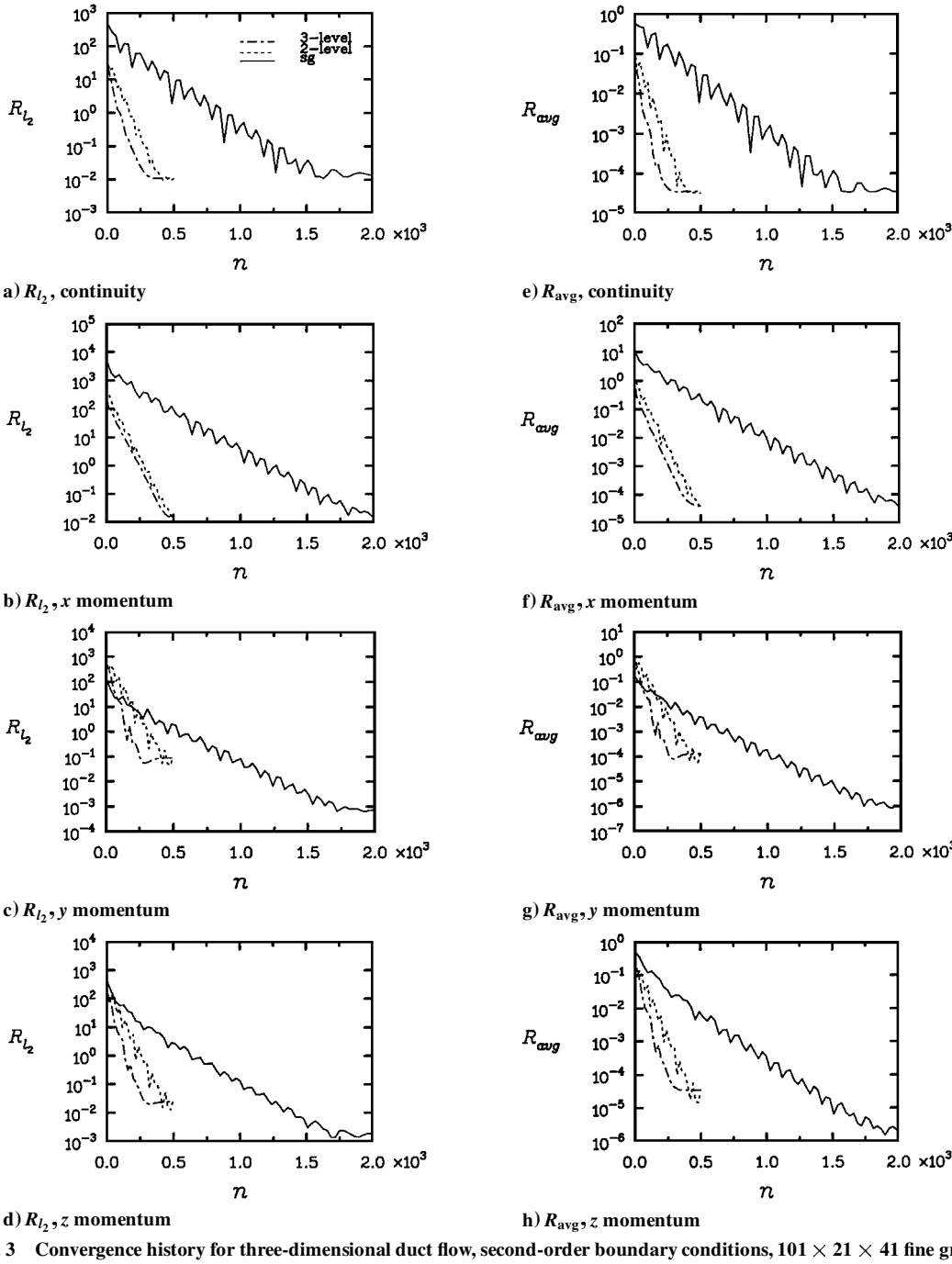


a) $R_{l_2}$, continuity

e) $R_{\text{avg}}$, continuity

b) $R_{l_2}$, $x$ momentum

f) $R_{\text{avg}}$, $x$ momentum

c) $R_{l_2}$, $y$ momentum

g) $R_{\text{avg}}$, $y$ momentum

d) $R_{l_2}$, $z$ momentum

h) $R_{\text{avg}}$, $z$ momentum

**Fig. 3 Convergence history for three-dimensional duct flow, second-order boundary conditions, 101 × 21 × 41 fine grid.**

analysis are used to study multigrid performance in this work, following Ibraheem and Demuren.[19]

The Beam and Warming ADI scheme formulated earlier can be represented in the operator form

$$N\Delta Q^n = -L = -\Delta t R^n \tag{11}$$

**Single-Grid Stability Analysis**

The convergence characteristics of the described scheme can be examined by using a von Neumann-type Fourier analysis method. This is performed by letting the step-by-step solution have the form

$$Q^n = U_0 \lambda^n e^{I i\theta_x} e^{I j\theta_y} e^{I k\theta_z} \tag{12}$$

Thus, Eq. (11), where $\hat{K} = \hat{N} - \hat{L}$, reduces to a complex generalized eigenvalue problem of the form[11]

$$\hat{K}x = \lambda \hat{N}x \tag{13}$$

The solution of this equation over only the high-frequency range $\pi/4 \leq |\Theta| < \pi/2$ yields the smoothing factor $\lambda_{\mu\text{-sg}} = \max(|\lambda|)$. The smoothing factor measures the effectiveness of the relaxation scheme in reducing high-frequency modes.

**Bigrid Stability Analysis**

Considering all the various steps involved in the MG process, the error equation per MG cycle can be written as[19]

$$\begin{aligned} e^{n+1} &= S_2^{\nu^2}\left(\boldsymbol{I} - I_H^h L_H^{-1} I_h^H L_h\right) S_1^{\nu^1} e^n \\ &= S_2^{\nu^2} K S_1^{\nu^1} e^n \\ &= M e^n \end{aligned} \tag{14}$$

where

$$K = \boldsymbol{I} - I_H^h L_H^{-1} I_h^H L_h$$

$$M = S_2^{\nu^2}\left(\boldsymbol{I} - I_H^h L_H^{-1} I_h^H L_h\right) S_1^{\nu^1}$$

The spectral radius of matrix $M$ is defined as the bigrid amplification factor, and it serves as a measure of the asymptotic convergence rate of MG methods:

$$\lambda_{\mu\text{-bg}} = \max\{\lambda[\hat{M}(\Theta)]\} \tag{15}$$

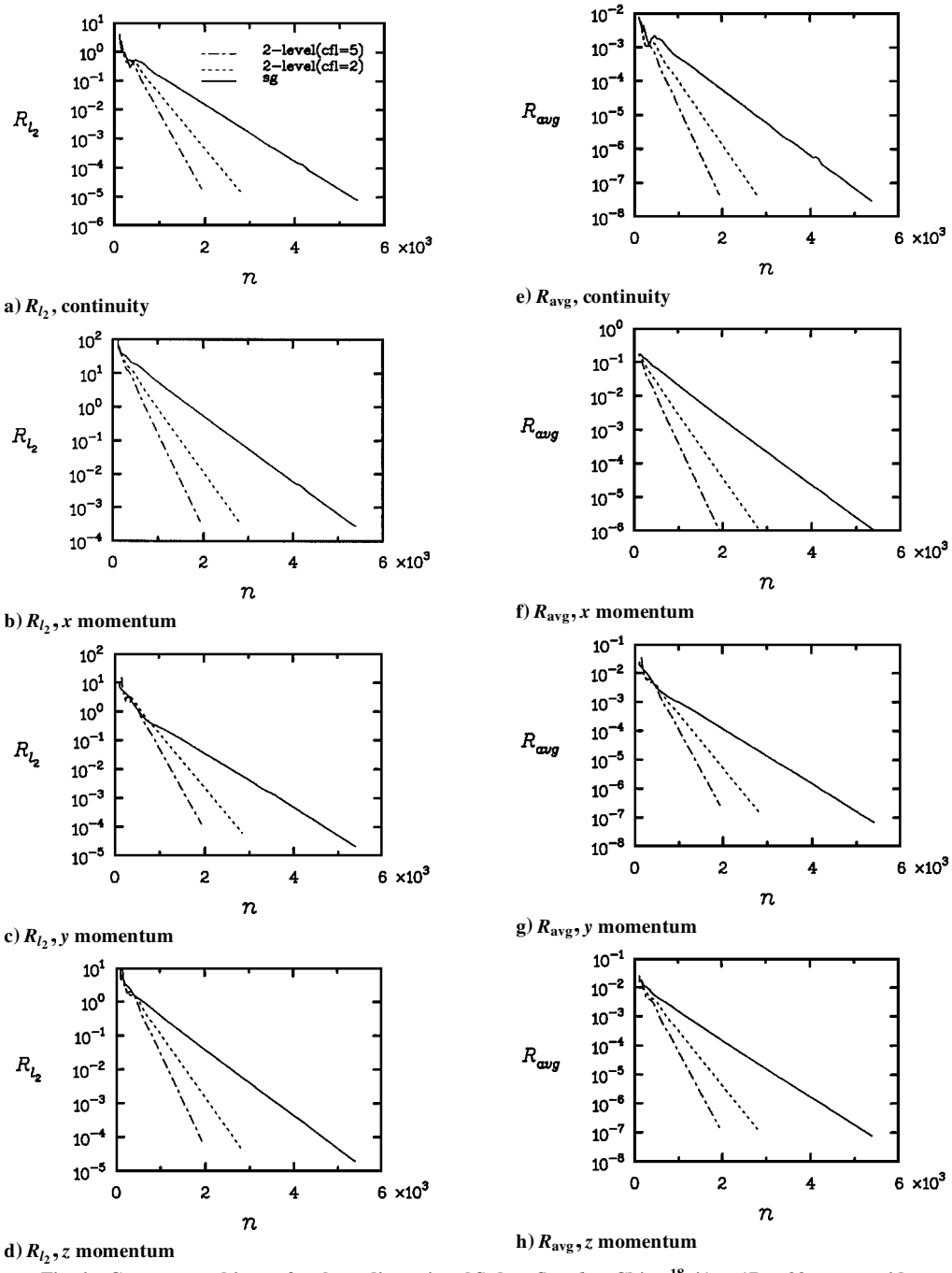


a) $R_{l_2}$, continuity

e) $R_{\text{avg}}$, continuity

b) $R_{l_2}$, $x$ momentum

f) $R_{\text{avg}}$, $x$ momentum

c) $R_{l_2}$, $y$ momentum

g) $R_{\text{avg}}$, $y$ momentum

d) $R_{l_2}$, $z$ momentum

h) $R_{\text{avg}}$, $z$ momentum

**Fig. 4 Convergence history for three-dimensional S-duct flow, $k$–$\varepsilon$ Chien,[18] 41 × 17 × 33 coarse grid.**

This factor predicts the performance of MG procedures better than the smoothing factor because it incorporates intergrid transfer processes. $\hat{M}(\Theta)$ in Eq. (15) is the Fourier representation of the matrix $M$. Note that, due to the aliasing process, low-frequency modes will couple with the coarse grid Fourier modes and, thus, for any $\Theta = \{\theta_x, \theta_y, \theta_z\}$ such that $-\pi/2 \leq \theta_x, \theta_y, \theta_z \leq \pi/2$, there exists a corresponding set of harmonics up to an integer multiple of $2\pi$. The bigrid amplification matrix $\hat{M}(\Theta)$ is an 8 × 8 block matrix of which each elemental block is a 5 × 5 matrix.[19]

The eigenvalues for the bigrid matrix $\hat{M}(\Theta)$ are computed from Eq. (15) over fixed Fourier modes to obtain the amplification factor. In the range $-\pi/2 \leq \Theta \leq \pi/2$, there are 16 modes selected.

#### Practical Convergence Rates

The practical convergence rate is computed in the numerical solution process as

$$\rho_{\text{mg}} = \left( \frac{\|R^{n2}\|}{\|R^{n1}\|} \right)^{1/(n2-n1)} \tag{16}$$

where $\|R^{n1}\|$ and $\|R^{n2}\|$ are the $l_2$ norm of the residuals at time levels $n1$ and $n2$, respectively. These time levels should be in the asymptotic convergence region.

## Results and Discussion

The test cases for the three-dimensional MG procedure are the two problems chosen to illustrate the original three-dimensional Proteus computer code,[13] namely, the developing laminar flow ($Ma = 0.1$, $Re = 60$) in a rectangular duct (aspect ratio = 5:1) and the turbulent flow ($Ma = 0.2$, $Re = 4 \times 10^4$) in an S duct. In the latter, computations were performed with the two-equation $k$–$\varepsilon$ turbulence model with low Reynolds number extensions proposed by Chien.[18] Computations were performed on the standard grid and on a coarser grid. Table 1 summarizes the test cases. The standard Courant–Friedrichs–Lewy (CFL) number of 10 is used on the finest grid in each case. The computed field solutions for these test cases agree very closely with experimental results,[20,21] as shown in Fig. 1.

The convergence rates of the single grid and the MG solutions for the developing duct flow are compared in Figs. 2 and 3. Coarse

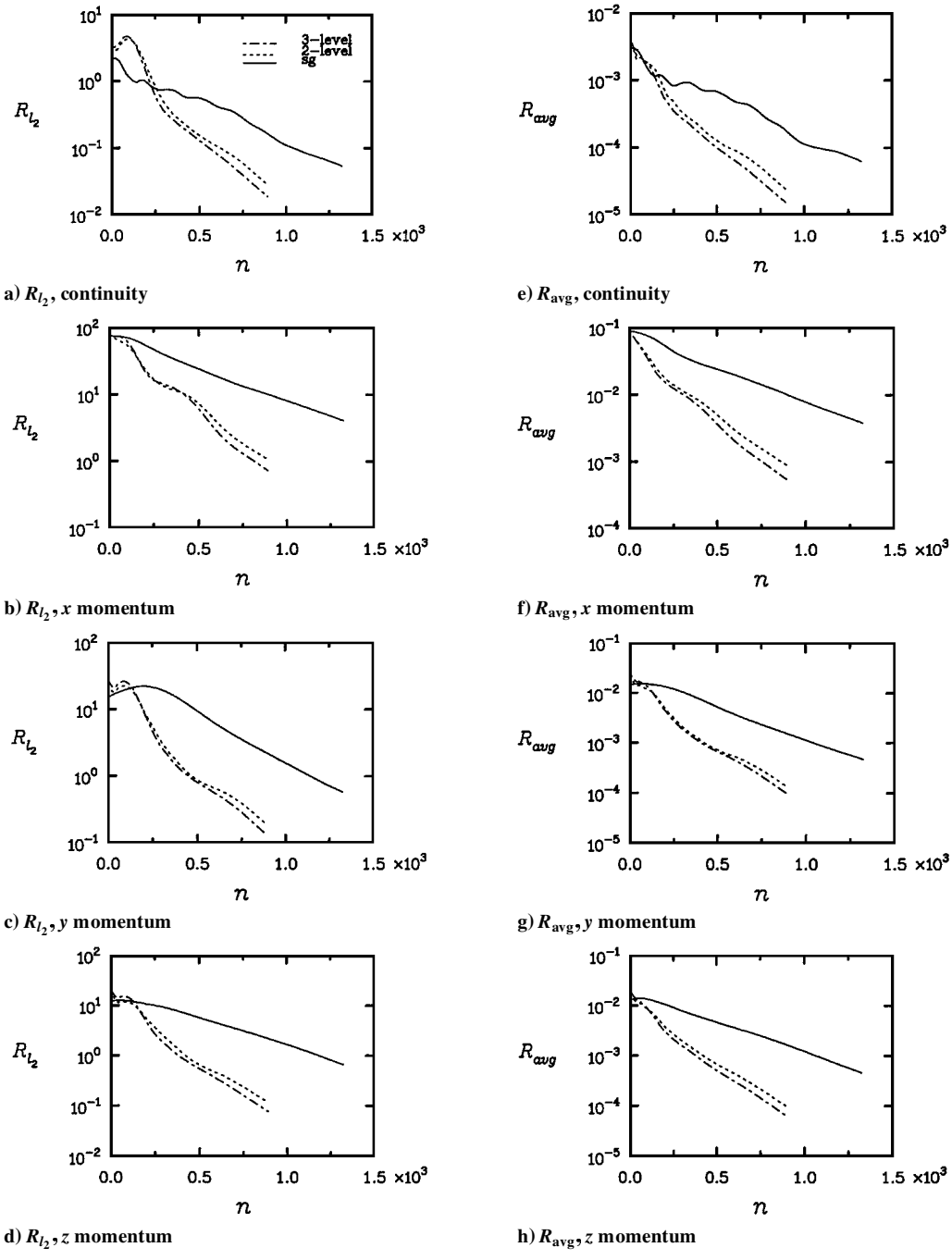


a) $R_{l_2}$, continuity

e) $R_{\text{avg}}$, continuity

b) $R_{l_2}$, $x$ momentum

f) $R_{\text{avg}}$, $x$ momentum

c) $R_{l_2}$, $y$ momentum

g) $R_{\text{avg}}$, $y$ momentum

d) $R_{l_2}$, $z$ momentum

h) $R_{\text{avg}}$, $z$ momentum

**Fig. 5 Convergence history for three-dimensional S-duct flow, $k$-$\varepsilon$ Chien,[18] 81 × 33 × 65 fine grid.**

grid results in forms of the $l_2$ norm and the average residuals of the continuity, $x$-, $y$-, $z$-momentum equations are presented in Fig. 2. It is clear that the MG solutions converged faster than the single-grid solution. The initial MG error is lower, because the full MG procedure provided better initial guesses on the fine grid by initially performing about 200 iterations on the coarsest grid. In this case the MG cycle was performed every third fine-grid iteration, so that the effective work units for each MG cycle is about 1.6. Thus, for a five-order-of-magnitude reduction in $x$-momentum residuals, there is about a 20% saving in total CPU time with the three-level MG procedure. The fine-grid results presented in Fig. 3 show even better savings. In this case, there is an MG cycle for every fine-grid iteration, so that the effective work units for each cycle is two. But for a five-order reduction in residuals the MG method (two or three level) requires about 400 iterations, whereas the single-grid method requires about 1700 iterations, i.e., more than 50% reduction in CPU time for the MG solutions. We note, however, that convergence of the three-level MG procedure appears to stagnate after about five-order reduction in residuals. We suspect that this is due to the implementation of the second-order boundary conditions. The problem can be eliminated by the use of local smoothing, as demonstrated by Ibraheem and Demuren.[19]

The residuals for the calculations of the turbulent S-duct flow are presented in Figs. 4 and 5. The convergence rates are much slower in this case in comparison to the laminar flow. Nevertheless, the three-level MG procedures showed much faster convergence, with a reduction of about 50% in CPU time to reach the same residual level. Coarse-grid computations are presented in Fig. 4. In this case only two-level MG cycles could be used. The effect of the CFL number used on the coarser grid is shown; the higher CFL number of five leads to faster convergence and, thus, is preferable, but it has been found to lead to instability and divergence in some problems. The computational saving in this case is about 30%, with a residual reduction of five orders in magnitude achieved in about 1700 iterations with the two-level MG procedure compared with 4800 iterations with the single-grid method. Corresponding fine-grid results are presented in Fig. 5. However, due to high computational costs, only residual reductions of two orders of magnitude with the MG

**Table 1 Description of test cases for three dimensions**

| Test case | Flow problem | Coarse grid | Fine grid |
|---|---|---|---|
| 1 | Rectangular duct, laminar | $41 \times 21 \times 21$ | $101 \times 21 \times 41$ |
| 2 | S duct, turbulent | $41 \times 17 \times 33$ | $81 \times 33 \times 65$ |

**Table 2 Convergence characteristics**

| Test case | Flow problem | Grid | $\lambda_{\mu-\mathrm{sg}}$ | $\lambda_{\mu-\mathrm{bg}}$ | $\rho_{\mathrm{mg}}$ |
|---|---|---|---|---|---|
| 1 | Rectangular duct, laminar | $41 \times 21 \times 21$ | 0.992 | 0.987 | 0.989 |
| | | $101 \times 21 \times 41$ | 0.974 | 0.974 | 0.975 |
| 2 | S duct, turbulent | $41 \times 17 \times 33$ | 0.991 | 0.992 | 0.997 |
| | | $81 \times 33 \times 65$ | 0.991 | 0.992 | 0.995 |

procedure are presented. The single-grid computation produces only one-order-of-magnitude reduction in residuals in the same number of iterations. By extrapolation, it is estimated that the savings in CPU time for the MG solution is about 40–50% in this case.

#### Convergence Rates

In the computations just presented, results of both the single-grid and the bigrid stability analyses are continuously used as guidelines. For instance, the asymptotic convergence rates that are computed from practical MG solutions of the various test cases are compared with the predictions from analyses in Table 2. For both flow problems, the smoothing factor and the bigrid factor predict the practical solutions reasonably. In general, however, the smoothing factor usually predicts MG performance poorly, especially at lower CFL numbers.[19]

## Concluding Remarks

The MG procedure has been developed for compressible viscous turbulent flow in three dimensions. Computed results from single-grid and bigrid Fourier stability predictions for the coupled Euler and Navier–Stokes equations served as a guide in the implementation of the MG method for the numerical computations. Convergence acceleration to steady state of various three-dimensional test cases ranging from laminar to turbulent flows were investigated for different geometries. In general, MG acceleration was found to be more effective in three-dimensional problems than in two-dimensional problems. Savings of up to 50% CPU time were obtained in several of the test cases.

## References

[1]Southwell, R. V., "Stress-Calculation in Frameworks by the Method of Systematic Relaxation of Constraints," *Proceedings of the Royal Society London*, Vol. 151A, No. 872, 1935, pp. 56–91.

[2]Stiefel, E. L., "Uber einige Methodern der Relaxationsrechnung," *Zeitschrift fuer Angewandte Mathematik und Physik*, Vol. 3, 1952, pp. 1–11.

[3]Federenko, R. P., "The Speed of Convergence of One Iterative Process," *Zhurnal Vychislitel'noi Matematiki i Matematicheskoi Fiziki*, Vol. 4, 1964, pp. 227–235.

[4]Bakhalov, N. S., "On the Convergence of a Relaxation Method with Natural Constraints on an Elliptic Operator," *Zhurnal Vychislitel'noi Matematiki i Matematicheskoi Fiziki*, Vol. 6, 1966, pp. 101–135.

[5]Brandt, A., "Multi-Level Adaptive Solutions to Boundary-Value Problems," *Mathematics of Computations*, Vol. 31, 1977, pp. 333–390.

[6]South, J. C., and Brandt, A., "The Multi-Grid Method: Fast Relaxation for Transonic Flows," *Advances in Engineering Science*, Vol. 4, 1976, pp. 1359–1368.

[7]Jameson, A., "Acceleration of Transonic Potential Flow Calculations on Arbitrary Meshes by the Multiple Grid Method," AIAA Paper 79-1458, 1979.

[8]McCarthy, D. R., and Reyhner, T. A., "Multigrid Code for Three Dimensional Transonic Flows," *AIAA Journal*, Vol. 20, 1982, pp. 45–50.

[9]Jameson, A., "Solution of the Euler Equations for Two-Dimensional Transonic Flow by a Multigrid Method," *Applied Mathematics Computations*, Vol. 13, No. 3, 1983, pp. 327–356.

[10]Mulder W. A., "Analysis of a Multigrid Method for the Euler Equations of Gas Dynamics in Two Dimensions," *Multigrid Methods, Theory, Applications and Supercomputing*, edited by S. F. McCormick, Lecture Notes in Pure and Applied Mathematics, Marcel Dekker, New York, 1988, pp. 467–478.

[11]Anderson, W. K., Thomas, J. L., and Whitfield, D. L., "Three-Dimensional Multigrid Algorithms for the Flux-Split Euler Equations," NASA TP-2829, 1988.

[12]Towne, C. E., Schwab, J. R., Benson, T. J., and Suresh, A., "PROTEUS Two-Dimensional Navier–Stokes Computer Code—Version 1.0, Volumes 1–3," NASA TM-102551-3, March 1990.

[13]Towne, C. E., Schwab, J. R., and Bui, T. R., "PROTEUS Three-Dimensional Navier–Stokes Computer Code—Version 1.0, Volumes 1–3," NASA TM-106341, Oct. 1993.

[14]Beam, R. M., and Warming, R. F., "An Implicit Scheme for the Compressible Navier–Stokes Equations," *AIAA Journal*, Vol. 16, 1978, pp. 393–402.

[15]Demuren, A. O., and Ibraheem, S. O., "On the Stability Analysis of Approximate Factorization Methods for 3-D Euler and Navier–Stokes Equations," *Numerical Heat Transfer, Part B*, Vol. 25, 1994, pp. 97–117; also NASA TM-106314, Oct. 1993.

[16]Steger, J. L., "Implicit Finite-Difference Simulation of Flow About Arbitrary Two-Dimensional Geometries," *AIAA Journal*, Vol. 16, 1978, pp. 679–686.

[17]Jameson, A., Schmidt, W., and Turkel, E., "Numerical Solutions of the Euler Equations by Finite Volume Methods Using Runge–Kutta Time-Stepping Schemes," AIAA Paper 81-1259, June 1981.

[18]Chien, K. Y., "Prediction of Channel and Boundary-Layer Flows with a Low-Reynolds-Number Turbulence Model," *AIAA Journal*, Vol. 20, 1982, pp. 33–38.

[19]Ibraheem, S. O., and Demuren, A. O., "On Bi-Grid Local Mode Analysis of Solution Techniques for 3-D Euler and Navier–Stokes Equations," *Journal of Computational Physics*, Vol. 125, 1996, pp. 354–377; also NASA TM-106749, Oct. 1994.

[20]Sparrow, E. M., Hixon, C.W., and Shavit, G., "Experiments on Laminar Flow Development in Rectangular Ducts," *Journal of Basic Engineering Science*, Vol. 89, 1967, pp. 116–124.

[21]Taylor, A. M. K. P., Whitelaw, J. H., and Yianneskis, M., "Developing Flow in S-Shaped Ducts," NASA CR 3550, May 1982.

D. S. McRae
*Associate Editor*